Nanotechnology Perceptions
ISSN 1660-6795
www.nano-ntp.com

Design, Synthesis, and Biological Evaluation of Some Diphenyl-1,2,4-Triazin-Linked Thiazole Derivatives to Treat Alzheimer's Disease

Omkar Singh[1,2], Vilas B. Ghawate[1,3], Prabhash Nath Tripathi[4], Pravin Kumar Singh[2], Ritesh Anand[5], Rajat Rai[2,6]

[1]Bhagawant University, Ajmer - 305004, Rajasthan, India
[2]Rahul Sankrityayan College of Pharmacy, Uttar Pradesh, India
[3]MES College of Pharmacy, Sonai, Maharashtra, India
[4]Meerut Institute of Engineering and Technology, Uttar Pradesh, India
[5]Amity Institute of Click Chemistry Research and Studies, Amity University, Uttar Pradesh, India
[6]Carreer Point University, Rajasthan, India
Email: omkarsingh85@gmail.com

One of the main causes of dementia in the world's aging population is AD, a progressive neurological disease. It is more important than ever for researchers to create novel therapeutic approaches to combat AD because of the massive threat it poses to world healthcare. For a more thorough knowledge of the underlying molecular mechanisms and pathophysiological pathways connected to the development and progression of AD, a thorough examination of the vast amount of data currently available is required. Cholinergic, Aβ, tau, excitotoxicity, oxidative stress, ApoE, CREB signaling pathways, insulin resistance, and other clinical and physiological symptoms are among the ones that are now understood. The benefits to cost ratio of cholinesterase therapy, the issue of decreased AChE selectivity over BChE, the BBB permeability of peptidic BACE-1 inhibitors, the difficulties that accompany the implementation of vaccination and immunization therapy, and the clinical failure of candidates related to newly available targets are some of the issues that need to be addressed. Nevertheless, these hypotheses have been criticized with multiple conflicting reports for their involvement in the progression of the disease.The current review sheds light on the various molecular mechanisms underlying the onset and progression of AD as well as prospective therapeutic approaches. It also clarifies perceptions with regard to the structural details of both conventional and novel

targets and how to make efficient use of computational techniques for target-specific inhibitor design. A new series of diphenyl-1,2,4-triazine linked thiazole derivatives were designed, synthesized, characterized, and evaluated as potential candidates to deal with Alzheimer's disease. Most of these compounds exhibited significant acetylcholinesterase inhibitory activities. These attributes highlight 7a-j as promising candidates for further studies directed to the development of novel drugs against Alzheimer's disease.

Keywords: Alzheimer's disease, Parkinson's disease, acetylcholine, AChE inhibitors, reactive oxygen species

1. Introduction

A mix of awareness, focus, acquaintance, memory, judgment, and decision-making contribute to cognition [1]. Cognitive impairment is a pathological condition associated with many neurodegenerative disorders such as Alzheimer's disease (AD), Parkinson's disease (PD), depression, and schizophrenia [2]. The neurotransmitters like acetylcholine (ACh), dopamine, serotonin, glutamate, etc. are responsible for regulating the cognitive symptoms and functionalities among this, ACh is essential for thinking processes since disorders of memory are triggered by its lack in the brain [3]. It is an illness that is associated with a variety of risk factors that can have severe repercussions in along with causing a tremendous financial and emotional strain on patients and their families [4]. Cognitive decline is one of the symptoms of AD, which nowadays affects 50 million people globally. By 2050, this figure will be more than triple to 152 million [5]. The condition ranks among the top eight detrimental to health globally and advances symptomatically from mild to severe [6] Parkinson's disease and Alzheimer's disease (AD[2,7,8,9] Neurotransmitters that control cognitive processes include glutamate [10], acetylcholine (ACh) [11], dopamine [12], serotonin [13], and others. Among these substances, acetylcholinestrase (AChE) hydrolyzes, ACh to produce choline and acetic acid [14]. ACh is a neurotransmitter that plays a significant role in controlling memory and learning processes. . Cognitive difficulties and short-term memory loss have been linked to low levels of ACh in the hippocampus, cortical geographic area, and basal forebrain [15,16] By creating AChE-Aβ complexes, AChE also causes the aggregation and deposition of Aβ fibrils, and affects cognitive function [17,18] Therefore, the two most promising strategies for slowing the progression of dementia are increasing ACh through AChE inhibition and preventing Aβ aggregation. Another harmful element brought on by an imbalance between the production of reactive oxygen species (ROS) and antioxidant enzymes is oxidative stress. Overproduction of ROS causes lipid peroxidation and protein oxidation, which in turn results in oxidative damage and compromised cognitive function. Aβ may also enter the mitochondria, increasing the production of free radicals and causing oxidative stress, according to research[19,20,21].

The USFDA has currently approved three AChE inhibitors (donepezil, rivastigmine, and galantamine) to treat AD symptoms; yet, these drugs do not actively prevent progression of the disease [22]. These medications use can be limited in the later stages of the disease due to a number of side effects, notably weakness, cramp in the muscles, and urine incontinence [23,24].

The clinical and physiological characteristics that are currently understood include insulin resistance, oxidative stress, cholinergic, tau, Aβ, excitotoxicity, ApoE, and CREB signaling

pathways. Nevertheless, these theories have been dismissed for their role in the progression of the disease in an assortment of findings that are conflicting. The benefits to cost ratio of cholinesterase therapy, the conundrum of AChE selectivity over BChE, the BBB permeability of peptidic BACE-1 inhibitors, obstacles associated with vaccination and immunization therapy implementation, and clinical failure of candidates related to newly available targets are just a few of the issues that call for attention. Methylfonate and tesofensine, a pair AChEIs that were found to be promising compounds to treat dementia in recent years, have been withdrawn from clinical trials since due to their poor CNS stability and toxicity [25,26,27]. Therefore, there is an unmet need to find new neurotherapeutic drugs to reduce AChE activity and alter the course of the disease.

2. RESULT AND DISCUSSION

2.1. Chemistry

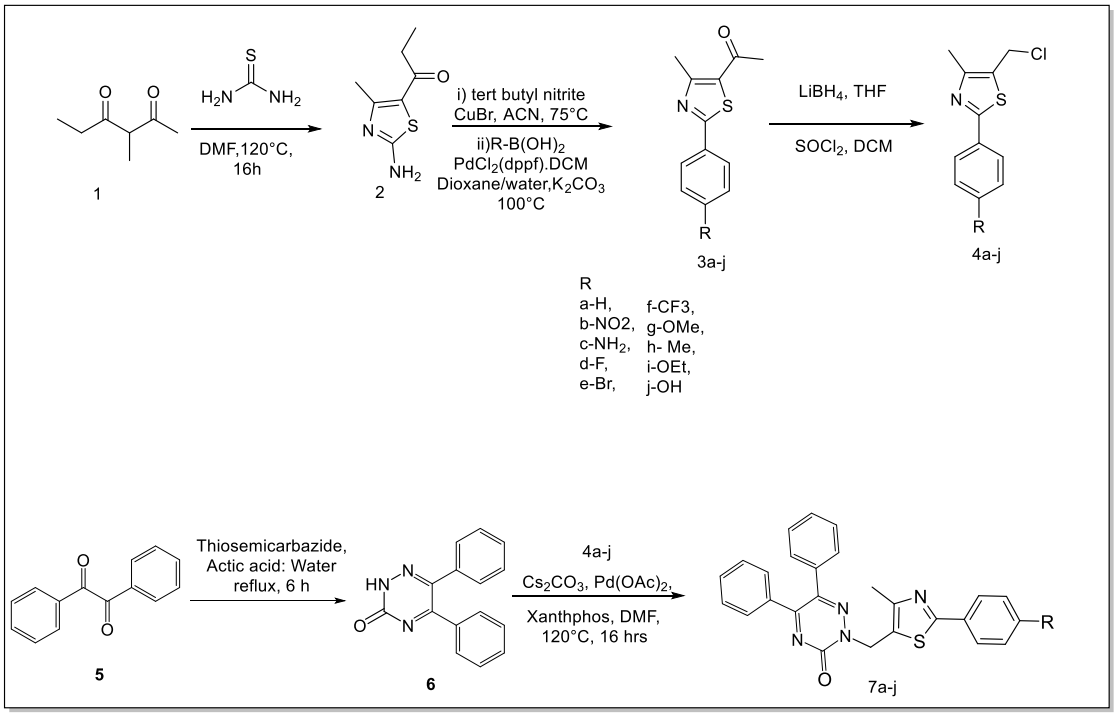

Scheme 1: Synthesis of diphenyl-1,2,4-triazine-linked thiazole derivatives.

The title compounds (7a -j) were prepared using the reaction sequence described in Scheme 1.

In the first step, 3-methylhexane-2,4-dione (1) is reacted with thiourea in the presence of DMF at 120°C for 16 h to give the 1-(2-amino-4-methylthiazol-5-yl)propan-1-one (2). Then, intermediate (3a-j) is took into acetonitrile with copper bromide and tertiary butyl nitrile at 75°C for 4-5 h and again reacted with the R-substituted boronic acid and potassium carbonate in the presence of dioxane/water under nitrogen. Added PdCl2(dppf).DCM complex catalyst at 100°C for 16 h to afford (3a-j). The compound (3a-j) is treated with lithium borohydride

solution (2M) in the presence of THF solvent. Quenched reaction with ice-cold water and extracted with ethyl acetate to afford crude compound which is further treated with thionyl chloride in the presence of 0°C for 2 h to afford intermediate (4a-j). Compound (6) reacted with thiazole derivatives (4a-j) in the presence of base $CsCO_3$ and using catalyst palladium acetate/xanthphos in the presence of 1,4-dioaxne solvent at 120°C for 16 h. The reaction mixture was monitored by TLC and after completion reaction was quenched with water and extracted with ethyl acetate. Combined organic layer and washed with saturated brine solution. Purified by column chromatography in 100-200 silica gel with 0-50% ethyl acetate in hexane to afford (7a-j).

2.2. Biological activity

2.2.1. In vitro Ellman assay

All the synthesized compounds (7a-7j) were evaluated by Ellman's colorimetric method on hAChE (acetylcholinesterase from human erythrocyte) and hBChE (butyrylcholinesterase from human serum) using donepezil as a reference standard (Table 1). With the exceptions of compounds 7a, 7c and 7j, inhibited hAChE (IC50 > 100). Among derivatives, compound 7g, 7h and 7i, bearing an electron-donating methoxy group, methyl group, showed significant hAChE inhibitory potential (pIC50 = 17.82 ± 4.89, 12.08 ± 3.73, 12.08 ± 3.73). Next, of the compounds 7b, 7e, 7f, in this series, which possess electron withdrawing groups (Nitro, bromo, trifloromethyl) on the phenyl ring, exhibited slightly diminished hAChE inhibitory activities compared to those of compounds which possess electron-donating groups. Among all the evaluated derivatives (7a – 7i), compound 7d, bearing a floro group, displayed the most significant hAChE inhibitory activity (IC50 = 2.34 ± 0.72). The enhanced lipophilicity of compound 7d due to its floro group may be the cause of its effective interactions with the active site residues of hAChE. Compounds 7d the only synthesized compounds that significantly inhibited hBChE. Ellman's colorimetric method on hAChE (acetylcholinesterase from human erythrocyte) and hBChE (butyrylcholinesterase from human serum) using donepezil as a reference standard (Table 1) was applied for evaluation of all the synthesized compounds (7a–7j)

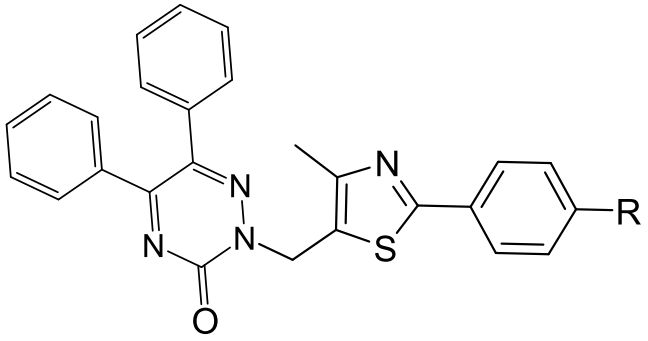

Table 1 [a]Selective index ratio = (BChE IC_{50})/(AChE IC_{50})

S. No	R	Compound code	eeAChE IC_{50} ± SDM (µM)	BChE IC_{50} ± SD (µM)	[a]SI ratio
1	-H	7a	>100	27 ± 4.02	-

2	$-NO_2$	7b	7.43 ± 0.59	>100	-
3	$-NH_2$	7c	>100	>100	-
4	-F	7d	2.34 ± 0.72	9.75 ± 3.75	4.03
5	-Br	7e	10.18 ± 2.89	31.57 ± 1.51	3.10
6	$-CF_3$	7f	5.27 ± 1.21	>100	-
7	OMe	7g	17.82 ± 4.89	>100	-
8	-Me	7h	12.08 ± 3.73	>100	-
9	-OEt	7i	10.25 ± 3.21	21.69 ± 4.28	2.12
10	-OH	7j	>100	>100	-
11	Donepezil		0.20 ± 0.01	-	-

2.2.2. Acute toxicity study

Healthy swiss albino mice (25–30 g) was taken for acute toxicity study of compound 7d following the OECD 423 guidelines. Monitoring for Several behavioral changes, cholinergic effects and toxic reactions, such as tremors, convulsions, salivation, diarrhea, sleep, lacrimation and feeding behavior, was done. After administration of test compound 7d no signs of any cholinergic side effects, and no toxicity or mortality was observed a significant safety margin has been shown by compound 7d.

2.2.3. In vivo Scopolamine-induced Y-maze-based memory study

Compound 7d was assessed for its ability to enhance learning and memory against a scopolamine-induced cognitive deficit. The results showed a significantly decreased (***$p < 0.001$) spontaneous alternation rate in scopolamine compared to the control. Treatment with compound 7d elicited a dose-dependent increase (2.5 mg/kg: ##$p < 0.01$; 5 and 10 mg/kg: ###$p < 0.001$) in the spontaneous alternation rate compared to scopolamine (Fig. 1). Additionally, the locomotive behavior of the scopolamine-treated mice did not change as confirmed by the non-significant changes in total arm entries among all groups (Fig. 2).

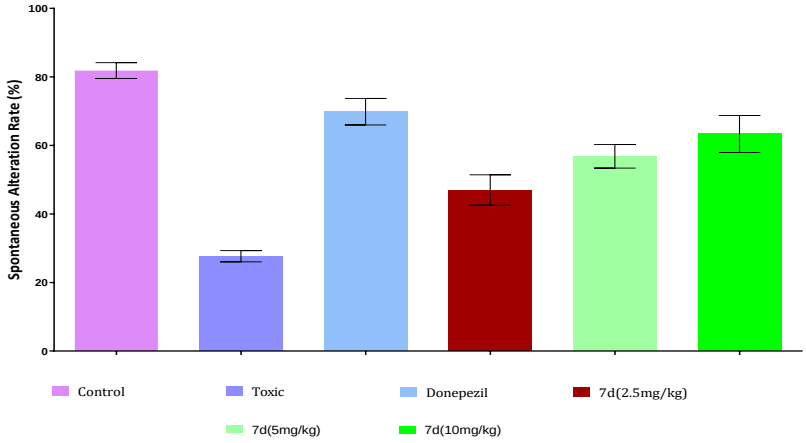

Figure 1. Spontaneous alternation rate compared to scopolamine

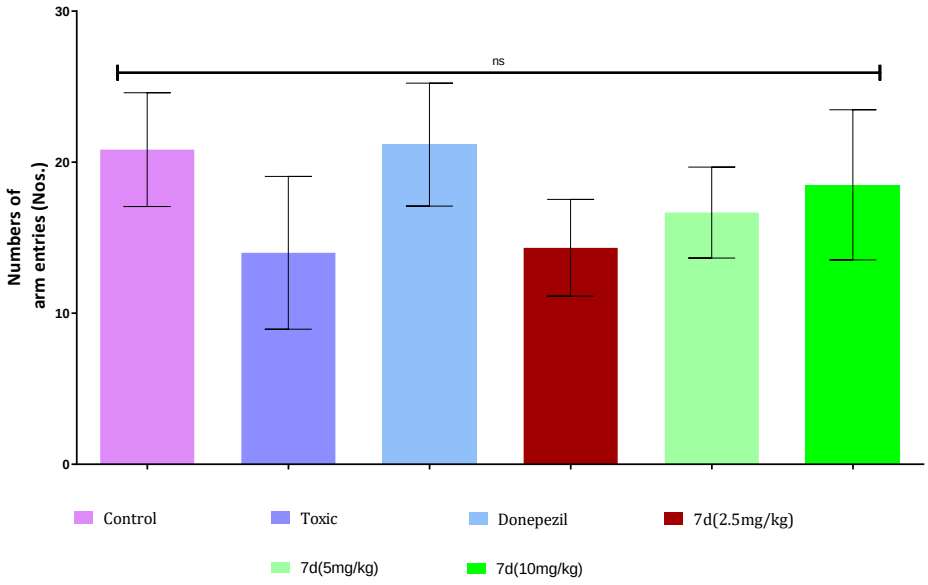

Figure 2. Non-significant changes in total arm entries among all groups

Effect of compound 7d (2.5, 5 and 10mg/kg) in the Y-maze test. (A) Spontaneous alterations rate; (B) Number of arm entries; Bars display values as mean ± SD (n=6) and analyzed by one-way ANOVA followed by Tukey's test; $p < 0.05$.

2.3. Computational Studies

2.3.1 Molecular docking study

Glide module of Schrödinger Maestro 2018–1 was used to to assess the binding affinity and pose stability of Compound 7d in the active sites of hAChE (PDB Code: 4EY7) for a molecular docking study. For validation of the docking parameters, the cocrystallized Aricept (donepezil) ligand was extracted and redocked in the hAChE grid. In the comperative study of the poses of the cocrystallized and redocked ligands using a superposition tool RMSD value was found to be 0.2 Å (Supp. Fig. 3).

Docked scores were found to be -9.878 kcal/mole for donepezil and −14.6 kcal/mole for Compound 7d . π-π stacking and polar interactions with His447 in the catalytic active site (CAS) was observed by napthyl group of Compound 7d. All PAS residues were interacted by Compound 7d through hydrophobic interactions (Tyr72, Tyr124, Trp286 and Tyr341) and electrostatic interactions (Asp74). Hydrophobic interactions with Trp86 and Phe338 and electrostatic interactions with the Glu202 residue were formed by Compound 7d at the anionic subsite. Compound 7d interacted with Gly121 and Gly122 and formed hydrophobic interactions with Ala204 at the oxyanion site.

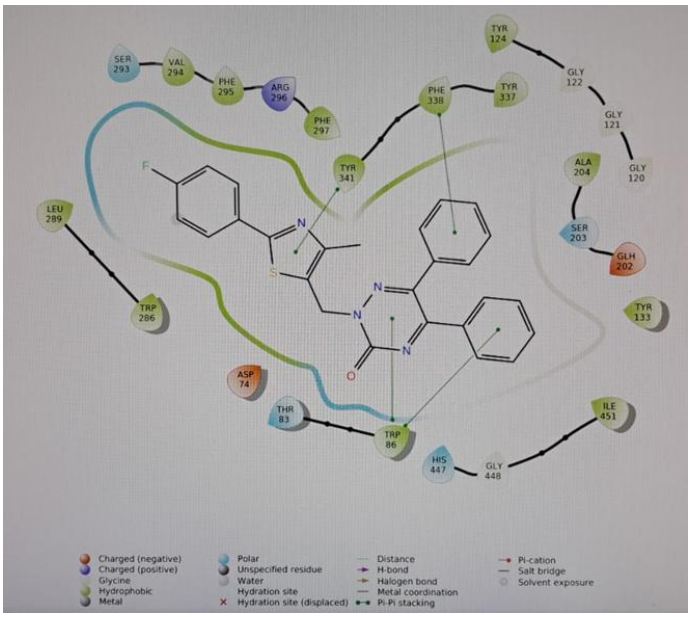

Figure 3. RMSD value was found to be 0.2 Å of compound 7d

2.3.2. Molecular dynamic study

A 30 nsec MD simulation was performed to affirm the binding pose stability of the Compound 7d -hAChE docked complex. The generated trajectories were utilized to produce simulation interaction diagrams, and the results were analyzed. The stability of the docked protein–ligand complex was determined by RMSD (root mean square deviation) and RMSF (root mean square fluctuation) calculations. The protein–ligand RMSD showed initial fluctuations up to 6.25 nsec before stabilizing. The docked complex was compared to the reference protein backbone structure, which was stabilized and found to be within 1–3 Å (Fig. 8).

The structural stability of the protein and Compound 7d was also evaluated based on the RMSF value, which was found to be < 3 Å and confirmed the absence of overall local changes along the protein chain and positions of the atoms in the ligand. The results of the MD simulations were analyzed using simulation interaction diagrams. The representation of the interaction analysis through stacked bar charts showed the normalized value of the interaction fractions over the course of the trajectory. For example, the value of 0.6 suggests that a specific interaction was maintained for 60% of the simulation period.

The results suggested that the interaction between Compound 7d and the PAS residues remained intact throughout the simulation. The detailed analysis showed that Compound 7d interacted through H bonding, hydrophobic interactions and salt-bridge formation with Tyr72, Asp74, Tyr124, Trp286 and Tyr341 in the PAS with interaction fractions of 0.52, 0.68, 0.69, 0.74 and 0.81, respectively.

Furthermore, interaction analysis was represented graphically (Fig. 4) to show the H-bonding and hydrophobic interactions that existed for more than 20% of the total simulation run time. The results showed that the nitrogen atom of 2-AP exhibited H-bonding interactions with

Asp74 (20%) and Trp286 (22%) at the PAS. Additionally, Asp74 showed H-bonding interactions (21%) with the –NH linker. Furthermore, the results suggested a hydrophobic interaction between Compound 5d and the Tyr341 residue at the PAS. The results of the MD simulation analysis were also analyzed as a function of time (Fig. 5).

The top panel of a timeline representation shows the total number of specific contacts (H-bonding, hydrophobic, ionic, and water bridge interactions) between the protein and the ligand over the course of the simulation run. The bottom panel shows the interactions of individual amino acid residues in each trajectory frame during the simulation run. Some residues formed more than one specific interaction with the ligand, which was represented by a darker shade of orange according to the scale at the right of the plot.

Overall, the results of the MD simulation analysis suggested stable and effective interactions between Compound 7d and the PAS, and the results were found to be in agreement with those of the PI displacement assay.

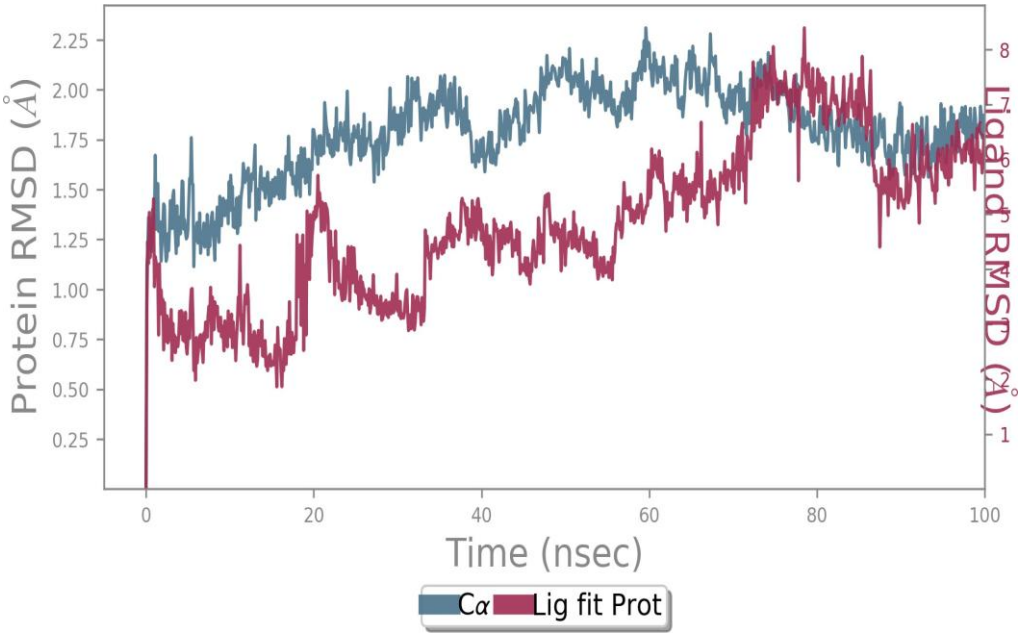

Figure 4. Protein-Ligand contacts

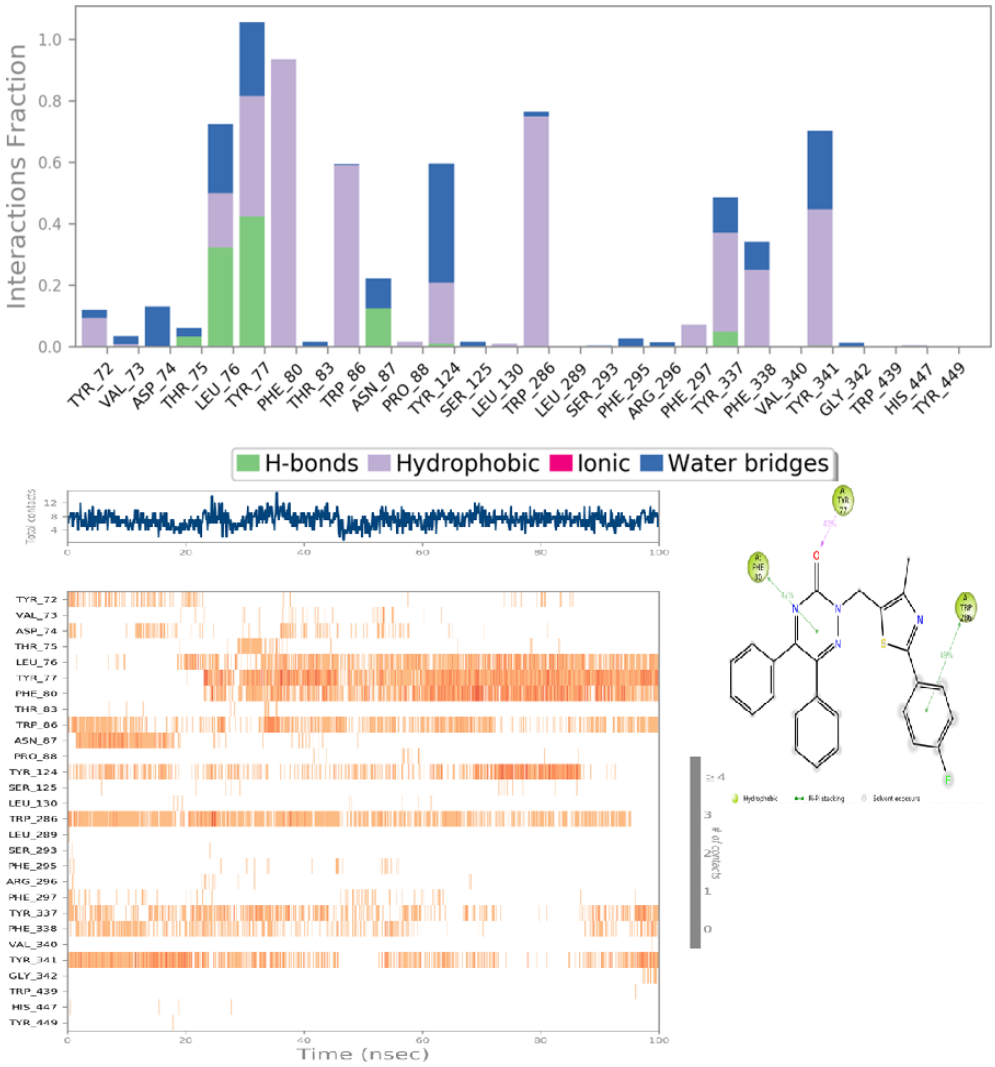

Figure 5. MD simulation analysis

2.3.2.1. Protein-Ligand RMSD

The Root Mean Square Deviation (RMSD) is used to measure the average change in displacement of a selection of atoms for a particular frame with respect to a reference frame. It is calculated for all frames in thetrajectory. The RMSD for frame x is:

$$RMSD_x = \sqrt{\frac{1}{N}\sum_{i=1}^{N}(r_i'(t_x)) - r_i(t_{ref}))^2}$$

where N is the number of atoms in the atom selection; t_{ref} is the reference time, (typically the

first frame is used as the reference and it is regarded as time t=0); and r' is the position of the selected atoms in frame x

after superimposing on the reference frame, where frame x is recorded at time t_x. The procedure is repeatedfor every frame in the simulation trajectory.

2.3.2.2. Protein RMSD

The above plot shows the RMSD evolution of a protein (left Y-axis). All protein frames are first aligned on the reference frame backbone, and then the RMSD is calculated based on the atom selection.

Monitoring the RMSD of the protein can give insights into its structural conformation throughout the simulation. RMSD analysis can indicate if the simulation has equilibrated — its fluctuations towards the end of the simulation are around some thermal average structure. Changes of the order of 1-3 Å are perfectly acceptable for small, globular proteins. Changes much larger than that, however, indicate that the protein is undergoing a large conformational change during the simulation. It is also important that your simulation converges — the RMSD values stabilize around a fixed value. If the RMSD of the protein is still increasing or decreasing on average at the end of the simulation, then your system has not equilibrated, and your simulation may not be long enough for rigorous analysis.

3. Conclusion

Herein, we designed and synthesized a novel set of multitarget-di reacted molecules with both a triazine moiety and a substituted 1,3,4-thiazole ring for the treatment of cognitive dysfunctions. Among all the synthesized derivatives, floro group-bearing compound 7d showed the highest in vitro hAChE inhibitory activity (IC50=2.34) with a noncompetitive enzyme inhibition (Ki=0.17µM). In vivo behavioral studies revealed that compound 7d (10mg/kg) significantly reversed the scopolamine-induced cognitive dysfunctions in mice as evaluated by Y-maze and passive avoidance tests. The computational studies corroborated the pharmacological outcomes owing to the effective interactions between compound 7d and the active site residues of PAS. Thus, this study indicated that multi targeted 5,6- diphenyl-1,2,4-triazine-3-thiazole derivatives are potential scaffolds for the treatment of dementia with compound 7d as a promising lead for further research.

4. Experimental Section

4.1. Chemistry

All the chemicals and reagents were obtained from Sigma-Aldrich (India), Cayman chemicals (USA), Avra Synthesis (India) and were utilized without purifying until stated. The melting points were calculated on Stuart melting point apparatus (SMP10) using capillary tubes, and are reported as uncorrected. The reaction progress was monitored using a pre-coated silica G60 aluminum sheet (Merck, Germany) using n-hexane/ Ethyl acetate (EtOAc) (80:20 v/v) as mobile phase followed by TLC visualization accomplished on UV light with various visualizing agents i.e., Dragendorff's reagent,

and/or iodine vapors. Merck silica gel was employed for column chromatography. 1 H and 13C NMR spectra were documented using DMSO-d6 as a solvent on a 500 MHz FT NMR spectrophotometer (Bruker, USA). Mass spectra was recorded on X500R QTOF (Applied Biosystems) mass spectrophotometer in positive ion mode.

4.1.1. General procedure of synthesis of (4a-j)

In the first step, 3-methylhexane-2,4-dione (1) is reacted with thiourea in the presence of DMF at 120°C for 16 h to give the 1-(2-amino-4-methylthiazol-5-yl)propan-1-one (2). Then, intermediate (3a-j) is took into acetonitrile with copper bromide and tertiary butyl nitrile at 75°C for 4-5 h and again reacted with the R-substituted boronic acid and potassium carbonate in the presence of dioxane/water under nitrogen. Added PdCl2(dppf).DCM complex catalyst at 100°C for 16 h to afford (3a-j). The compound (3a-j) is treated with lithium borohydride solution (2M) in the presence of THF solvent. Quenched reaction with ice-cold water and extracted with ethyl acetate to afford crude compound which is further treated with thionyl chloride in the presence of 0°C for 2 h to afford intermediate (4a-j). Further, the synthesized derivatives were established using the state of art spectroscopy.

Compound 4a

Yield: 500 mg; 87.82%; m.p. 222-224 ^{o}C; ^{1}H-NMR shifts (DMSO, δ ppm): 7.51-8.05 (m, 5H), 4.67 (s, 2H) 2.25 (s, 3H).

Compound 4b

Yield: 400 mg; 87.82%; m.p. 222-224 ^{o}C; ^{1}H-NMR shifts (DMSO, δ ppm): 8.03-8.27(m, 4H) 4.68 (s, 2H), 2.23 (s, 3H.

Compound 4c

Yield: 300 mg; 87.82%; m.p. 222-224 ^{o}C; ^{1}H-NMR shifts (DMSO, δ ppm): 6.59-7.80 (m, 4H), 5.25 (brs, 2H) 4.64 (s, 2H), 2.25 (s, 3H).

Compound 4d

Yield: 350 mg; 87.82%; m.p. 222-224 ^{o}C; ^{1}H-NMR shifts (DMSO, δ ppm): 7.31-8.78 (m, 4H), 4.64 (s, 2H), 2.23 (s, 3H).

Compound 4e

Yield: 300 mg; 87.82%; m.p. 222-224 ^{o}C; ^{1}H-NMR shifts (DMSO, δ ppm): 7.64-7.87 (m, 4H), 4.63 (s, 2H), 2.22 (s, 3H).

Compound 4f

Yield: 300 mg; 87.82%; m.p. 222-224 ^{o}C; ^{1}H-NMR shifts (DMSO, δ ppm): 7.65-7.97 (m, 4H), 4.65 (s, 2H), 2.21 (s, 3H).

Compound 4g

Yield: 300 mg; 87.82%; m.p. 222-224 ^{o}C; ^{1}H-NMR shifts (DMSO, δ ppm): 7.15-8.19 (m, 4H), 4.65(s, 2H), 3.81(s, 3H).

Compound 4h

Yield: 300 mg; 87.82%; m.p. 222-224 ^{o}C; ^{1}H-NMR shifts (DMSO, δ ppm): 7.12-7.89(m, 4H), 4.65(s, 2H), 2.35(s, 3H), 2.21(s, 3H).

Compound 4i

Yield: 350 mg; 87.82%; m.p. 222-224 ^{o}C; ^{1}H-NMR shifts (DMSO, δ ppm): 7.03-7.98 (m, 4H), 4.65(s, 2H), 4.05(q, 2H), 2.21(s, 3H), 1.35(t, 3H).

Compound 4j

Yield: 350 mg; 87.82%; m.p. 222-224 ^{o}C ^{1}H-NMR shifts (DMSO, δ ppm): 9.67 (brs, 1H), 7.56-7.60 (Aromatic, 4H), 4.65(s, 2H), 2.35(s, 3H). 2.21(s, 3H), LCMS: 90%, ^{13}C-NMR shifts (DMSO, δ ppm): 14.3, 42.5, 114.6, 128.1, 129.2, 134.9, 152.0, 159.4, 168.8

4.1.2. General procedure of synthesis of 5,6-diphenyl-1,2,4-triazine-3-thiol (6):

5,6- diphenyl-1,2,4-triazine-3-thiol (6) was prepared with minor variations to the previously described procedure. Benzil (5) was dissolved in glacial acetic acid and then added to a hot water mixture of thiosemicarbazide and further reflux for 4 h. The precipitate obtained was recrystallized with ethanol to obtain orange-yellow color crystals of the desired compound.

Yield: 5.27g; 87.82%; m.p. 222-224 ^{o}C; ^{1}H-NMR shifts ($CDCl_3$, δ ppm): 7.27-7.57 (m, 10H). 11.78 (b, NH, 1H); LCMS: 95%, ^{13}C-NMR shifts ($CDCl_3$, δ ppm): 179.24, 160.73, 146.66, 132.22, 130.28, 130.10, 129.86, 129.40, 128.74, 128.60, 128.39.

4.1.3. General procedure of synthesis of ethyl 4,5-diphenyl-2H-imidazole-2-carboxylate (7a-j):

Compound (6) reacted with thiazole derivatives (4a-j) in the presence of base $CsCO_3$ and using catalyst palladium acetate/xanthphos in the presence of 1,4-dioaxne solvent at 120°C for 16 h. The reaction mixture was monitored by TLC and after completion reaction was quenched with water and extracted with ethyl acetate. Combined organic layer and washed with saturated brine solution. Purified by column chromatography in 100-200 silica gel with 0-50% ethyl acetate in hexane to afford (7a-j).

Compound 6

^{1}H-NMR (400 MHz, DMSO-d_6), δ- 16.7 (brs, 1H), 7.41-7.96 (m, 6H). LCMS: 80%.

Compound 7a

Yield: 400 mg; 87.82%; m.p. 222-224 ^{o}C; ^{1}H-NMR (400 MHz, DMSO-d_6), δ- 8.05 (d, J = 7.5 Hz, 2H), 7.80 (d, J = 7.6 Hz, 4H), 7.50-8.40 (m, 9H), 4.18 (s, 2H), 2.15 (s, 3H). LCMS: 80%.

Compound 7b

Yield: 300 mg; 87.82%; m.p. 222-224 ^{o}C; ^{1}H-NMR (400 MHz, DMSO-d_6), δ- 8.32 (d, J = 7.5 Hz, 2H), 8.23 (d, J = 7.5 Hz, 2H), 7.79 (d, J = 7.6 Hz, 4H), 7.50-7.40 (m, 6H), 4.18 (s, 2H), 2.15 (s, 3H). LCMS: 90%.

Compound 7c

Yield: 250 mg; 87.82%; m.p. 222-224 ºC; ^{1}H-NMR (400 MHz, DMSO-d_6), δ- 7.79 (d, J = 7.6 Hz, 2H), 7.51-7.41 (m, 10H), 6.58 (d, J = 7.6 Hz, 2H), 4.18 (s, 2H), 2.16 (s, 3H). LCMS: 91%.

Compound 7d

Yield: 200 mg; 87.82%; m.p. 222-224 ºC; ^{1}H-NMR (400 MHz, DMSO-d_6), δ- 8.29 (t, J = 5.0 Hz, 2H), 7.79 (d, J = 7.6 Hz, 2H), 7.51 (d, J = 7.6 Hz, 4H), 7.47 (d, J = 7.6 Hz, 2H), 7.41 (m, 2H), 7.30 (m, 2H), 4.18 (s, 2H), 2.16 (s, 3H). LCMS: 95%. ^{13}C-NMR shifts ($CDCl_3$, δ ppm): 15.2, 32.5, 116.5, 127.6, 128.7, 129.7, 135.2, 135.9, 138.3, 150.1, 151.9, 157.3, 162.0, 168.6, 170.5.

Compound 7e

Yield: 200 mg; 87.82%; m.p. 222-224 ºC; ^{1}H-NMR (400 MHz, DMSO-d_6), δ- 7.79 (d, J = 7.6 Hz, 2H), 7.68-7.66 (dd, J = 7.6 Hz, 4H), 7.51 (d, J = 7.6 Hz, 4H), 7.47 (d, J = 7.6 Hz, 2H), 7.41 (m, 2H), 4.19 (s, 2H), 2.16 (s, 3H). LCMS: 94%.

Compound 7f

Yield: 200 mg; 87.82%; m.p. 222-224 ºC; ^{1}H-NMR shifts ($CDCl_3$, δ ppm): 7.27-7.94 (m, 10H), 4.22 (s, 2H), 2.21 (s, 3H), LCMS: 91%. ^{13}C-NMR shifts ($CDCl_3$, δ ppm): 14.2, 32.5, 123.4, 125.7 127.6, 128.7, 129.7, 131.2, 135.9, 138.3, 146.1, 150.1 152.1, 156.0, 168.6, 170.8

Compound 7g

Yield: 200 mg; 87.82%; m.p. 222-224 ºC; ^{1}H-NMR shifts ($CDCl_3$, δ ppm): 7.02-8.15 (m, 10H), 4.22 (s, 2H), 3.81 (s, 3H), 2.21 (s, 3H). LCMS: 90%. ^{13}C-NMR shifts ($CDCl_3$, δ ppm): 14.3, 32.5, 58.8, 114.8, 127.6, 128.7, 129.7, 135.9, 138.3, 150.1 152.1, 156.0, 160.7, 168.6, 170.8

Compound 7h

Yield: 100 mg; 87.82%; m.p. 222-224 ºC; ^{1}H-NMR shifts ($CDCl_3$, δ ppm): 7.22-7.95 (m, 10H), 4.22 (s, 2H), 2.34 (s, 3H), 2.21 (s, 3H). LCMS: 90%. ^{13}C-NMR shifts ($CDCl_3$, δ ppm): 14.3, 21.3, 32.5, 127.4, 127.7, 128.4, 129.5, 131.7, 135.9, 138.3, 140.4, 150.1 152.1, 156.0, 168.6, 170.8

Compound 7i

Yield: 100 mg; 87.82%; m.p. 222-224 ºC; ^{1}H-NMR shifts ($CDCl_3$, δ ppm): 7.03-8.15 (m, 10H), 4.21 (s, 2H), 4.05 (q, 2H), 2.34 (s, 3H), 2.21 (s, 3H), 1.34 (t, 3H). LCMS: 90%. ^{13}C-NMR shifts ($CDCl_3$, δ ppm): 14.5, 14.8, 32.5, 64.5, 114.9, 127.4, 128.2, 128.6, 129.5, 134.7, 135.9, 138.3, 150.1, 152.1, 156.0, 159.4, 168.6, 170.8

Compound 7j

Yield: 50 mg; 87.82%; m.p. 222-224 ºC; ^{1}H-NMR shifts ($CDCl_3$, δ ppm): 9.65 (brs, 1H), 6.86-7.84 (m, 10H), 4.21 (s, 2H), 2.21 (s, 3H), LCMS: 90%. ^{13}C-NMR shifts ($CDCl_3$, δ ppm): 14.5, 32.5, 114.9, 127.4, 128.2, 129.2, 135.9, 138.3, 150.1, 152.1, 156.0, 159.1, 168.4, 170.2

4.2. Biological activity

4.2.1. In vitro Ellman assay

The Ellman's assay procedure was used to evaluate the AChE level [28]. To start the reaction, first added 25µL of supernatant, 150µL of 0.1M sodium phosphate buffer (pH 7.4), and 100µL of 1mM DTNB to a 96-well microplate. After 10 minutes of fermentation, added 20µL of 7.5mM ATCI. At 412 nm, the reaction mixture's absorbance was measured. The substrate hydrolyzed/min/mg protein was used to express the AChE inhibitory potency results.

4.2.2. Acute oral toxicity study. In healthy Swiss albino mice, the substance 6g had been evaluated for acute oral toxicity according with OECD-423, 2001 criteria. The mice received doses of up to 500 mg/kg of the chemical (6g), and they were monitored for adverse responses or death for a total of 14 days.[29].

4.2.3. Y-maze test. The y-maze apparatus is a three-arm maze that is often used for determining mice' short-term and instantaneous working memory. Scopolamine hydrobromide was given through the abdomen (i.p.) to all mouse groups except the control group 30 minutes after the seventh day of therapy. For five minutes, the mice in each group were housed in the middle of the y-maze to reconnoiter the three arms. In order to capture the total number of arm entries, activities were monitored in the camera. The formula for calculating the "memory improvement score" is % alternations = (number of alternations/(total arm entries–2)).×100[30].

4.3. Computational studies

4.3.1. Molecular docking

The study of compound 6g's consensual binding and active site interactions on AChE (PDB Code: 1EVE) was done by molecular docking studies[31]. The Protein Preparation Wizard program was used to create the protein's crystal structure. First, bond ordering and hydrogen bonds were assigned. Prime was used to add the missing side chains and loops. Using the Epik at pH 7.0 ± 2.0, the heteroatom states were created and the water molecules that were more than 5Å away from the heteroatoms were eliminated. The protein structure was also optimized using the PROPKA method at pH 7.0 and minimized at restrained minimization by maintaining the convergence heavy atoms RMSD at 0.30Å. The generated protein structure was utilized for receptor grid generation in order to identify the active sites around the distance of 10X10X10 Å from the centroid of the co-crystallized ligand (donepezil). The stable conformers of ligands (compound 6g and do nepezil) were created using the LigPrep module, and these were then docked using the Glide XP module of Schrödinger Maestro 2018-1. The Glide XP visualizer tool was used to conduct detailed interaction analyses.

4.3.2. Molecular dynamics

To confirm the binding stability and pattern of the compound 6g-AChE complex utilizing Desmond, a 20 nsec molecular dynamics simulation run was conducted. The system was first constructed using the system builder, which used a cubic simulation box of the TIP3P explicit water system to create a virtual water environment. The box wall and the protein–ligand complex had to be at least 10Å apart. The system had been neutralized by adding counter ions, and 0.15M NaCl was added to create an isosmotic salt environment. The system's energy was

minimized by using a conjugate gradient algorithm with a maximum of 2000 interactions and a convergence criterion of 1 kcal/mol/Å. The system's temperature and pressure were set to 300K and 1.013 atmospheric bar, respectively, and a 20 nsec simulation run with periodic boundary conditions under an isothermal-isobaric ensemble (NPT) was performed out subsequent energy reduction.

References

[1] A. A. Geronikaki et al., "Design of new cognition enhancers: from computer prediction to synthesis and biological evaluation," J Med Chem, vol. 47, no. 11, pp. 2870–2876, 2004.

[2] R. Etcheberrigaray and D. L. Alkon, "Methods for Alzheimer's Disease treatment and cognitive enhancement," Nov. 30, 2004, Google Patents.

[3] Y. Xu et al., "Neurotransmitter receptors and cognitive dysfunction in Alzheimer's disease and Parkinson's disease," Prog Neurobiol, vol. 97, no. 1, pp. 1–13, 2012.

[4] Y. Huang and L. Mucke, "Alzheimer mechanisms and therapeutic strategies," Cell, vol. 148, no. 6, pp. 1204–1222, 2012.

[5] L. C. Howarth, "Dementia friendly memory institutions," The International Journal of Information, Diversity, & Inclusion, vol. 4, no. 1, pp. 20–41, 2020.

[6] G. Cornutiu, "The epidemiological scale of Alzheimer's disease," J Clin Med Res, vol. 7, no. 9, p. 657, 2015.

[7] P. N. Tripathi et al., "Biphenyl-3-oxo-1, 2, 4-triazine linked piperazine derivatives as potential cholinesterase inhibitors with anti-oxidant property to improve the learning and memory," Bioorg Chem, vol. 85, pp. 82–96, 2019.

[8] P. Srivastava et al., "Design and development of some phenyl benzoxazole derivatives as a potent acetylcholinesterase inhibitor with antioxidant property to enhance learning and memory," Eur J Med Chem, vol. 163, pp. 116–135, 2019.

[9] S. K. Shrivastava et al., "Design and development of novel p-aminobenzoic acid derivatives as potential cholinesterase inhibitors for the treatment of Alzheimer's disease," Bioorg Chem, vol. 82, pp. 211–223, 2019.

[10] A. Blokland, "Acetylcholine: a neurotransmitter for learning and memory?," Brain Res Rev, vol. 21, no. 3, pp. 285–300, 1995.

[11] J. Kulisevsky, "Role of dopamine in learning and memory: implications for the treatment of cognitive dysfunction in patients with Parkinson's disease," Drugs Aging, vol. 16, pp. 365–379, 2000.

[12] P. Jäkälä, J. Puoliväli, M. Björklund, E. Koivisto, and P. Riekkinen Jr, "Activation of acetylcholine receptors and 5-HT2 receptors have additive effects in the suppression of neocortical high-voltage spindles in aged rats," Psychopharmacology (Berl), vol. 132, no. 3, pp. 270–280, 1997.

[13] W. Vogel, D. M. Broverman, J. G. Draguns, and E. L. Klaiber, "The role of glutamic acid in cognitive behaviors.," Psychol Bull, vol. 65, no. 6, p. 367, 1966.

[14] P. Sharma, P. Srivastava, A. Seth, P. N. Tripathi, A. G. Banerjee, and S. K. Shrivastava, "Comprehensive review of mechanisms of pathogenesis involved in Alzheimer's disease and potential therapeutic strategies," Prog Neurobiol, vol. 174, pp. 53–89, 2019.

[15] J. A. Horel, "The neuroanatomy of amnesia: A critique of the hippocampal memory hypothesis," Brain, vol. 101, no. 4, pp. NP1–NP1, 1978.

[16] A. Easton, V. Douchamps, M. Eacott, and C. Lever, "A specific role for septohippocampal acetylcholine in memory?," Neuropsychologia, vol. 50, no. 13, pp. 3156–3168, 2012.

[17] G. Johnson and S. W. Moore, "The peripheral anionic site of acetylcholinesterase: structure, functions and potential role in rational drug design," Curr Pharm Des, vol. 12, no. 2, pp. 217–

225, 2006.
[18] G. V De Ferrari, M. A. Canales, I. Shin, L. M. Weiner, I. Silman, and N. C. Inestrosa, "A structural motif of acetylcholinesterase that promotes amyloid β-peptide fibril formation," Biochemistry, vol. 40, no. 35, pp. 10447–10457, 2001.
[19] K. Jomova, D. Vondrakova, M. Lawson, and M. Valko, "Metals, oxidative stress and neurodegenerative disorders," Mol Cell Biochem, vol. 345, pp. 91–104, 2010.
[20] R. Liu et al., "Reversal of age-related learning deficits and brain oxidative stress in mice with superoxide dismutase/catalase mimetics," Proceedings of the National Academy of Sciences, vol. 100, no. 14, pp. 8526–8531, 2003.
[21] W. R. Markesbery, "Oxidative stress hypothesis in Alzheimer's disease," Free Radic Biol Med, vol. 23, no. 1, pp. 134–147, 1997.
[22] L. Peauger et al., "Donepezil-based central acetylcholinesterase inhibitors by means of a 'bio-oxidizable' prodrug strategy: design, synthesis, and in vitro biological evaluation," J Med Chem, vol. 60, no. 13, pp. 5909–5926, 2017.
[23] S. Thompson, K. L. Lanctôt, and N. Herrmann, "The benefits and risks associated with cholinesterase inhibitor therapy in Alzheimer's disease," Expert Opin Drug Saf, vol. 3, no. 5, pp. 425–440, 2004.
[24] M. Mehta, A. Adem, and M. Sabbagh, "New Acetylcholinesterase Inhibitors for Alzheimer′ s Disease," Int J Alzheimers Dis, vol. 2012, no. 1, p. 728983, 2012.
[25] J. López-Arrieta and L. Schneider, "Metrifonate for Alzheimer's disease," Cochrane database of systematic reviews, no. 2, 2006.
[26] T. B. Ali, T. R. Schleret, B. M. Reilly, W. Y. Chen, and R. Abagyan, "Adverse effects of cholinesterase inhibitors in dementia, according to the pharmacovigilance databases of the United-States and Canada," PLoS One, vol. 10, no. 12, p. e0144337, 2015.
[27] R. K. Harrison, "Phase II and phase III failures: 2013–2015," Nat Rev Drug Discov, vol. 15, no. 12, pp. 817–818, 2016.
[28] G.L. Ellman, K.D. Courtney, V. Andres Jr, R.M. Featherstone, A new and rapid colorimetric determination of acetylcholinesterase activity, Biochem. Pharmacol. 7 (2) (1961) 88–95
[29] S.K. Shrivastava, B.K. Patel, P.N. Tripathi, P. Srivastava, P. Sharma, A. Tripathi, A. Seth, M.K. Tripathi, Synthesis, evaluation and docking studies of some 4-thiazolone derivatives as effective lipoxygenase inhibitors, Chem. Pap. (2018) 1–15.
[30] A. Wolf, B. Bauer, E.L. Abner, T. Ashkenazy-Frolinger, A.M. Hartz, A comprehensive behavioral test battery to assess learning and memory in 129S6/Tg2576 mice, PLoS ONE 11 (1) (2016) e0147733.
[31] G.Kryger, I. Silman, J.L. Sussman, Structure of acetylcholinesterase complexed with E2020 (Aricept®): implications for the design of new anti-Alzheimer drugs, Structure 7 (3) (1999) 297–307.